ARTICLE

Ultrafast Carrier Dynamics in CdSe/CdS/ZnS Quantum Dots

Guan-xin Yao[a,b], Zai-xi Fu[b], Xian-yi Zhang[b], Xian-feng Zheng[b], Xue-han Ji[b], Zhi-feng Cui[a,b*], Hong Zhang[c*]

a. Anhui Institute of Optics and Fine Mechanics, Chinese Academy of Sciences, Hefei 230031, China
b. Institute of Atomic and Molecular Physics, Anhui Normal University, Wuhu 241000, China
c. Van't Hoff Institute for Molecular Sciences, University of Amsterdam, Nieuwe Achtergracht 166, 1018 WV Amsterdam, Netherlands

(Dated: Received on May 24, 2011; Accepted on July 18, 2011)

The intra- and inter-band relaxation dynamics of CdSe/CdS/ZnS core/shell/shell quantum dots are investigated with the aid of time-resolved nonlinear transmission spectra which are obtained using femtosecond pump-probe technique. By selectively exciting the core and shell carrier, the dynamics are studied in detail. Carrier relaxation is found faster in the conduction band of the CdS shell (about 130 fs) than that in the conduction band of the CdSe core (about 400 fs). From the experiments it is distinctly demonstrated the existence of the defect states in the interface between the CdSe core and the CdS shell, indicating that ultrafast spectroscopy might be a suitable tool in studying interface and surface morphology properties in nanosystems.

Key words: CdSe/CdS/ZnS quantum dot, Femtosecond pump-probe technique, Ultrafast carrier dynamics, Transient transmission spectrum

I. INTRODUCTION

Semiconductor nanocrystals or quantum dots (QDs) are quasi-zero-dimensional nanoscale materials where the motion of carriers is restricted in all three directions, and have a unique electronic structure different from that of the atomic and bulk materials [1]. The QDs' optical, electronic and transport properties depend on their size and shape. Through the size controlling, the band-gap energy can be tuned in a broad spectral range and carrier relaxation paths can be manipulated *e.g.* trapping, radiative, and nonradiative decays [2−5]. Obviously, comprehension of the photophysical properties of these materials is important for the development of highly efficient light-emitting nanocrystalline devices or solar cells based on QDs.

The II-VI CdSe QD systems are the most thoroughly investigated nanoscale materials [6]. By coating a proper shell on the bare core, *e.g.* CdS, ZnS, and ZnSe coated on CdSe [7, 8], the surface states may be reduced, leading to enhanced fluorescence quantum yield, and carrier relaxation path may also be altered [1, 9, 10]. There are two types of such core/shell semiconductor nanocrystal systems, denoted as type I and type II, respectively. For type I systems, the band-gap of the core material is smaller than that of the shell material, with the band edges of the core confined inside the band-gap of the shell, while for type II system, the band alignments of the core and the shell are staggered [11, 12]. In the core/shell system, the carrier relaxation could involve several processes such as phonon relaxation, surface and defect states trapping, Auger relaxation, *etc.* Generally, these processes are ultrafast within femtosecond to picosecond order [13]. In this sense, femtosecond laser spectroscopy has been proven to be a powerful tool in unravelling those ultrafast carrier dynamics in core/shell QDs systems. Be more specific, the ultrafast spectroscopic techniques are suitable to follow energy relaxation, population decay, optical gain, ionization dynamics, and biexciton interactions [1, 11−16].

Recently, ultrafast carrier dynamics have been extensively investigated on the nanoscale materials for core/shell structures which have two configurations of "dot-in-a-rod" and "rod-in-a-rod" [11, 12, 17−22]. Cretí *et al.* studied ultrafast processes and the effect of the shell thickness on stimulated emission and photoinduced absorption transitions in CdSe/CdS/ZnS core/shell nanorods by femtosecond pump-probe spectroscopy [22]. According to their study, the decay time of the higher energy states is shorter in the core (200 fs) than in the core/shell samples (500 fs) from transient transmission difference spectra, and also the density of such states depends on the shell thickness. They claimed that the interface defects are negligible for thin shells. Lupo *et al.* investigated the transient bleaching and absorption of the asymmetric core/shell CdSe/CdS nanorods using pump-probe technique [11]. They observed ultrafast carrier relaxation and identified hole

*Authors to whom correspondence should be addressed. E-mail: zfcui@mail.ahnu.edu.cn, h.zhang@uva.nl

localization dynamics with time constant of 650±80 fs, and an intense bleaching signal in the CdS spectral which was assigned to the delocalization of the electronic wave upon pumping of the CdSe core. Recently, Deka *et al.* studied ultrafast dynamics of CdSe/CdS nanorods and CdSe/CdS/ZnS double shell nanorods, employing pump-probe and time-resolved photoluminescence spectroscopy [12]. They confirmed that the presence of the ZnS shell reduced the presence of trap states at the CdS surface, and consequently led to an increased probability for charge carrier decay at CdSe emitting states and therefore to an increased quantum efficiency.

In the present work, the carrier dynamics of type-I CdSe/CdS/ZnS core/shell/shell quantum dots dispersed in chloroform solution was studied using femtosecond pump-probe technique. Tuning the femtosecond excitation wavelength the carriers initially were either restricted in the core area or extended into different shells as well. To the best of our knowledge, the ultrafast carrier dynamics about CdSe/CdS/ZnS double shell quantum dots have not been reported yet. It is found that the relaxation processes of carriers are subject to the initial preparation. Our results indicate that the carrier relaxation is very fast when carriers in the core and shell are all excited-comparable with the width of laser pulse (130 fs), whereas it is slower (about 400 fs) when the carriers are prepared in the core only. This fast relaxation is ascribed to the trapping of the defects in the interface between the CdSe core and the CdS shell.

II. EXPERIMENTS

A. Preparation of CdSe/CdS(3 ML)/ZnS(3 ML) QDs

The CdSe/CdS(3 ML)/ZnS(3 ML) double shells QDs was synthesized given elsewhere [23].

1. Chemicals

Cadmium oxide (99.99%), sulfur (99.98%, powder), zinc oxide (99.99% powder), 1-octadecene (ODE, 90%), oleic acid (OA, 90%), tri-octylphosphine (TOP), and oleylamine (OAm) selenium powder (99.5%, 100 mesh), were purchased from Alfa.

2. Synthesis of CdSe core nanocrystals

In a typical reaction, a mixture of 0.2 mmol CdO powder, 0.5 mmol of OA, 3 mL ODE, and 1 mL OAm were loaded into three-neck flask, then the reaction mixture was evacuated for 1 h and heated to 280 °C under Ar-flow to form an optically clear solution. A solution containing 0.1 mmol Se dissolved in 2.0 g of TOP was injected into the reaction flask. After the injection, the temperature was adjusted to 250 °C for 1 min. After this time the heating mantle was removed and cooled down to room temperature.

3. Preparation of the precursor solution of shell materials

The zinc precursor and cadmium precursor solution were prepared by dissolving ZnO and CdO in oleic acid and ODE at 300 °C, respectively. The sulfur precursor solution was prepared by dissolving sulfur in ODE at 180 °C. All the solutions were freshly prepared under Ar-atmosphere. For each shell growth, a calculated amount of a given precursor solution was injected with a syringe using standard air-free procedures. For the calculations of the amount of precursor solutions, the amount of the injection solution for each monolayer can be deduced from a calculation of the number of concentric volume as described in literature [17].

4. Preparation of the core/shell nanocrystals with different shells

The method of preparing core/shell nanocrystals was similar to that reported in literature [23]. A typical reaction for synthesis of CdSe/CdS/ZnS nanocrystals was performed as follows. 0.15 μmol CdSe dissolved in hexane (0.2 mL), 3 mL ODE and 1 mL of OAm were loaded into a 50 mL reaction vessel, heated to 100 °C under vacuum for 1 h. Subsequently, the solution was heated to 245 °C where the shell growth was performed for growth of shell materials by SILAR method. Finally, the reaction solution was cooled down to room temperature. For purification 10 mL of hexane were added and by-products were removed by successive methanol extraction until the methanol phase was clear.

B. Femtosecond pump-probe setup

The femtosecond transient absorption experiment was based on a Spectra-Physics Hurricane Titanium: Sapphire regenerative amplifier system (see Fig.1). The optical system of the Hurricane includes a seeding laser (Mai Tai), a pulse stretcher, a Ti:Sapphire regenerative amplifier, a Q-switched pumps laser (Evolution), and a pulse compressor. The 800 nm output of the laser was typically 1 mJ/pulse (130 fs) at a repetition rate of 1 kHz. A full-spectrum setup based on an optical parametric amplifier (Spectra-Physics OPA 800) as pump and residual fundamental light (800 nm, 150 μJ/pulse) from the pump OPA was used for white light generation. The OPA was used to generate excitation pulses at 320 and 380 nm about 10 $\mu J/cm^2$ as the pump pulses of pump-probe experiments. After the residual fundamental light was passed over a delay line (Physic In-

DOI:10.1088/1674-0068/24/06/640-646

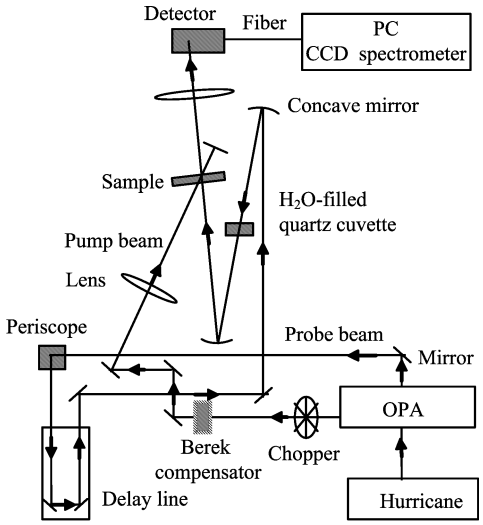

FIG. 1 Femtosecond pump-probe setup.

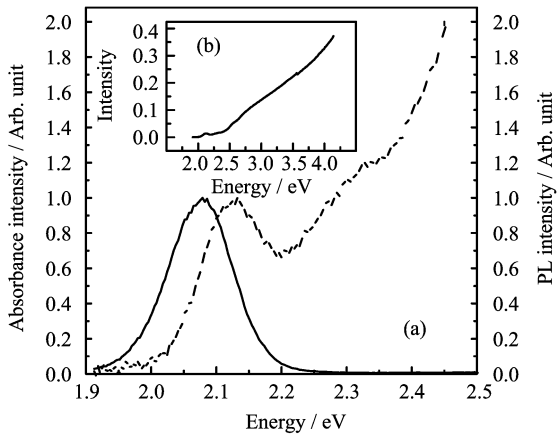

FIG. 2 (a) The normalized steady-state absorption spectra (dashed-line) and PL spectra (solid-line). Excitation was at 380 nm. (b) The entire steady-state absorption spectra. Two spectra are normalized for comparison.

strument, M-531DD, time window of 3.6 ns, maximal resolution of 1.2 fs/step), and focused into a H_2O-filled quartz cuvette of 2 mm path length (Hellma) to generate broad band spectrum-white light to be the probe pulses in the pump-probe experiments. The pump pulse is linearly polarized at the magic angle (54.7°) with respect to the probe by a Berek polarization compensator, then the two pulses were focused onto the same spot in the sample, which were placed into quartz cuvettes of 2 mm path length (Hellma) and stirred with a "stirring finger" to avoid local heating and decomposition by the laser beams. The angle between the pump and the probe beams was typically 7°−10°. At last, the probe pulse was coupled into a CCD spectrometer (Ocean Optics, PC2000) by an optical fiber. In order to minimize frequency chirp effect, the probe pulse was collected and focused onto the sample only by mirrors. Through the chopper, which was placed in the pump pulse, the intensity I (or I_0) of the probe beam after passing the sample in the excited (or unexcited) sample was obtained.

The transmission change ΔT is proportional to the absorption change ΔA in the small signal limit,

$$\frac{I - I_0}{I} = \frac{\Delta T}{T} \tag{1}$$

$$\Delta T = T^* - T \tag{2}$$

where T^* and T are the transmission of the probe beam in the excited and unexcited samples, respectively. The transient transmission ($\Delta T/T$) spectra can thus be obtained by recording transient absorption ($-\Delta A$) spectra using a CCD spectrometer. Further, the time-resolved nonlinear transmission spectra, *i.e.*, $\Delta T/T$ kinetic traces or $-\Delta A$ kinetic traces, can be collected with standard lock-in detection in the present experimental set-up. All the measurements are performed at room temperature, with the CdSe/CdS(3 ML)/ZnS(3 ML) QDs dispersed in chloroform solution.

III. RESULTS AND DISCUSSION

A. Steady-state absorption and PL spectra

Figure 2 gives the steady-state absorption and CdSe/CdS(3 ML)/ZnS(3 ML) photoluminescence (PL) spectra. The absorption spectra show a wide absorption band in the ultraviolet and visible region (Fig.2(b)), and the first excitonic absorption peak is at 2.14 eV (580 nm). The PL spectra (FWHM 120 meV) show only a band-edge fluorescence peak at 2.08 eV (598 nm) and its maximum is shifted from the first excitonic absorption peak by 60 meV.

According to the position of the first excitonic absorption peak of the sample, the average diameter of a QD can be estimated from the equation [24]:

$$D = 1.6122 \times 10^{-9}\lambda^4 - 2.6575 \times 10^{-6}\lambda^3 + 1.6242 \times 10^{-3}\lambda^2 - 0.4277\lambda + 41.57 \tag{3}$$

where D (in unit of nm) is the diameter of the nanocrystal sample, and λ (in unit of nm) is the wavelength of the first excitonic absorption peak of the corresponding sample. In this case the average diameter of the CdSe core is deduced to about 3.9 nm. The lattice constant a is 583.2 pm for the CdS and 540.93 pm for the ZnS, respectively [25], thus the d_{111} is 0.34 nm for CdS and 0.31 nm for ZnS using $d_{111}=\sqrt{3}a/3$. The thickness is calculated about 1.02 nm for the CdS shell and 0.93 nm for the ZnS shell (1 ML=d_{111}), respectively.

The shift of the band-edge luminescence peak relative to the first excitonic absorption peak may come from two possible causes. The first one is the presence of strong electron-phonon interaction or defects states (localized states), which are involved in the band-edge emission, and the second is the effect of the electric field of many electron-hole pairs formed in each particle under high pump intensity [26−28]. In our experi-

DOI:10.1088/1674-0068/24/06/640-646

TABLE I Time constants of $\Delta T/T$ kinetic traces fitted with a multi-exponential decay with pumping at 320 nm.

	$\bar{\tau}_{\rm rise}$/ps	$\bar{\tau}_1$/ps	$\bar{\tau}_2$/ps	$\bar{\tau}_3$/ps	$\bar{\tau}_4$/ps
X_1	0.86±0.02(−)	0.33±0.02(+)		189±9(+)	1244±150(+)
X_2	0.52±0.02(−)	0.21±0.02(+)	33±3(+)	124±16(+)	1441±374(+)
X_3	0.46±0.02(−)	0.27±0.02(+)	18±1(+)	159±14(+)	1488±269(+)
X_4	0.39±0.02(−)	0.21±0.02(+)	16±1(+)	106±9(+)	1277±374(+)

The signs of the pre-exponential factors are given in brackets.

ments, the average number $\langle n\rangle$ of electron hole pair per CdSe/CdS/ZnS particle can be expressed by the following formula [1]:

$$\langle n\rangle = j_p\sigma_0 \tag{4}$$

where j_p and σ_0 (in unit of cm^2) are the excitation fluence and the NC absorption cross section at the pump wavelength. In our experiments, the excitation fluence was 10 $\mu J/cm^2$ at 380 nm ($h\nu$<3.5 eV). So the σ_0 can be the following expression [1]:

$$\sigma_0 = 1.6\times 10^{-16}R^3 \tag{5}$$

where R (in unit of nm) is the radius of the nanocrystal sample. We can calculate that $\langle n\rangle$ of electron hole pair per CdSe/CdS/ZnS particle is about 0.02. Therefore, the possibility of the presence of multiexcitons and biexcitons is very small. We can then estimate that the peak shift is most probably due to the defect states which exist between the conduction band and the valence band of the CdSe core that are involved in the band-edge emission.

B. Time-resolved nonlinear transmission spectra

The time-resolved transmission spectrum is a function of excitation wavelength. The normalized transient transmission ($\Delta T/T$) of CdSe/CdS(3 ML)/ZnS(3 ML) at 4 ps delay relative to the pump pulse are recorded in Fig.3, with excitation at 320 and 380 nm, respectively. With a 320 nm (or 380 nm) pump, four absorption bleaching peaks can be recognized, as denoted in the Fig.3 by $X_1(Y_1)$, $X_2(Y_2)$, $X_3(Y_3)$, and $X_4(Y_4)$ bands that are centered at 2.10(2.10), 2.28(2.25), 2.55(2.53), and 2.67(2.67) eV, respectively. Among these bleaching bands, the X_1 (or X_4) band and the Y_1 (or Y_4) band are at the same position on energy. These bands may be ascribed to states filling effect.

In order to study ultrafast carrier dynamics of the different excited states of the sample, the kinetics of nonlinear $\Delta T/T$ of CdSe/CdS(3 ML)/ZnS(3 ML) QDs at the X_1, X_2, X_3, and X_4 bleaching bands with a 320 nm pumping and that at the Y_1, Y_2, Y_3, and Y_4 bleaching bands with a 380 nm pumping are shown in Fig.4 and Fig.5, respectively.

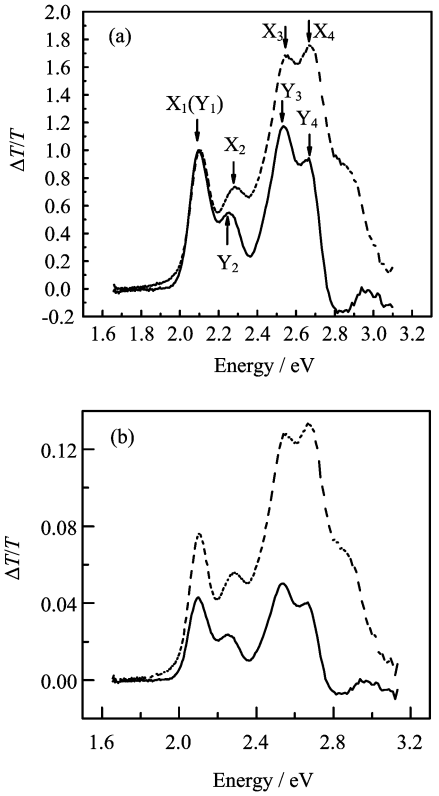

FIG. 3 (a) The normalized $\Delta T/T$ spectra recorded 4 ps after excitation, with an excitation fluence of 10 J/cm^2 at 320 nm (dashed line) and 380 nm (solid line). (b) The two $\Delta T/T$ spectra were not normalized.

In Fig.4, all the $\Delta T/T$ kinetic traces can be reasonably well fitted with multi-exponentials

$$y = y_0 + \sum A_i \exp\left(-\frac{t}{\tau_i}\right) \tag{6}$$

Time constants obtained from the fitting of the kinetic traces are listed in Table I. The pre-exponential factor of the first time constant is negative for all the four traces, and the time constant is defined as the signal's rise time ($\bar{\tau}_{\rm rise}$). From Table I, it is clear that the $\bar{\tau}_{\rm rise}$ increases from 390 fs (X_4 band) to 860 fs (X_1 band) as the probing photon energy decreases, whereas the decay times τ_i (i=1, 3, 4) are almost the same for these bands. It is worthy noting that there is no decay process

DOI:10.1088/1674-0068/24/06/640-646

TABLE II Time constants of $\Delta T/T$ kinetic traces fitted with a multi-exponential decay with pumping at 380 nm.

	$\bar{\tau}_{\rm rise}$/ps	$\bar{\tau}_1$/ps	$\bar{\tau}_2$/ps	$\bar{\tau}_3$/ps	$\bar{\tau}_4$/ps
Y_1	0.75±0.06(−)	0.27±0.09(+)		192±28(+)	1422±520(+)
Y_2	0.37±0.05(−)	0.22±0.05(+)		110±16(+)	1465±391(+)
Y_3	0.32±0.04(−)	0.16±0.04(+)		130±13(+)	1429±314(+)
Y_4	0.26±0.06(−)	0.15±0.08(+)	19±4(+)	114±36(+)	1316±403(+)

The signs of the pre-exponential factors are given in brackets

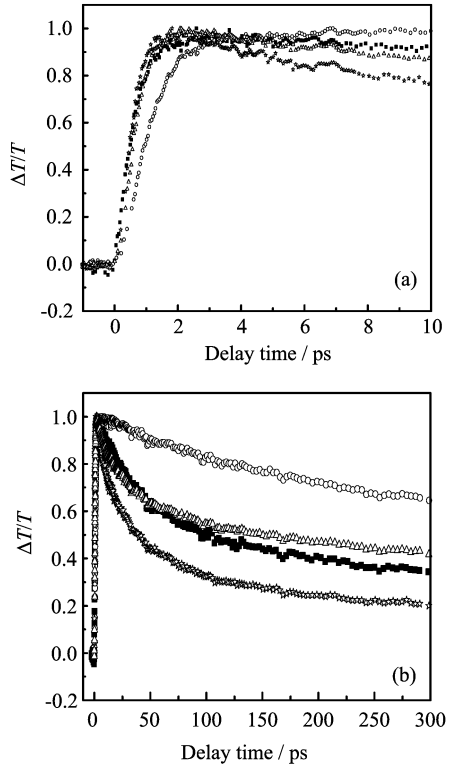

FIG. 4 Normalized bleaching $\Delta T/T$ kinetic traces at the X_1 (open circles), X_2 (solid squares), X_3 (open triangles), and X_4 (open stars) bands in the (a) 0−10 ps and (b) 0−300 ps range with pumping at 320 nm.

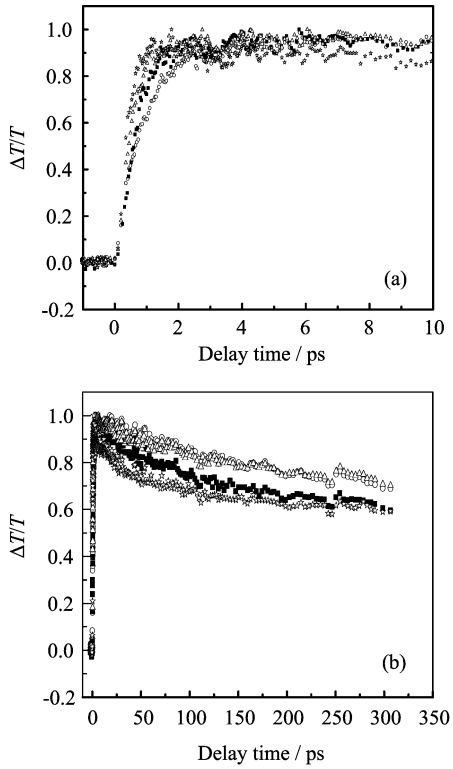

FIG. 5 Normalized bleaching $\Delta T/T$ kinetic traces at the Y_1 (open circles), Y_2 (solid squares), Y_3 (open triangles), and Y_4 (open stars) bands in the (a) 0−10 ps and (b) 0−300 ps range with pumping at 380 nm.

corresponding to τ_2 for the X_1 band.

Table II lists the time constants after fitting the experimental data under 380 nm pumping. Similar to the case with 320 nm pumping, the bleaching $\bar{\tau}_{\rm rise}$ increases from 260 fs (Y_4 band) to 750 fs (Y_1 band) as the probing photon energy decreases, but the rise time is also somewhat short compared with the counterpart under 320 nm pumping. The decay times $\tau_{1,3,4}$ are similar between the different bands, similar to the case of 320 nm pumping. However, We note that the decay time τ_2 is only observed for the Y_4 band, which is different from the case with 320 nm pumping.

C. Discussion

Tables I and II show that these $\Delta T/T$ kinetic traces are non-exponential which can be fitted with a four or five-exponential decay. This fact indicates that the dynamic processes might not be a simply one, instead it might contain several relaxation processes. The fastest decay time constants τ_1 in Tables I and II are about 150−300 fs and can be attributed to the trapping process in the interface between the CdSe core and the CdS shell. Also the τ_1 is observed at every bleaching band, and basically follows the same rule within a permissible error range, and the τ_1 of the higher bleaching band is less than $\tau_{\rm rise}$ of the lower bleaching band contiguous to the higher bleaching band under 320 or 380 nm

DOI:10.1088/1674-0068/24/06/640-646

pumping. Using the equation [21]:

$$\eta = \frac{1}{1 + \tau_1/\tau_{\rm rise}} \quad (7)$$

where η is the trapped carrier probability, we can estimate that the probability of the trapped carrier is about 70%. This indicates that a great deal of the carriers are trapped by defect states. In our experiments, the energies of the pumping photons are less than the gap energy of ZnS, and thus trapping process is shown up in every bleaching band. Considering the pump energy these defect states may exist between the CdSe core and the CdSe shell, and have energies between the $X_4(Y_4)$ and $X_1(Y_1)$ bands.

τ_2 was not observed at the X_1 band under 320 nm pumping (see Table I) and the decay time τ_2 was observed only at the Y_4 band under 380 nm pumping, which indicate that the X_1 band relaxation dynamics is different from the X_2, X_3, and X_4 bands of which the relaxation processes are identical basically under 320 nm pumping, and the relaxation processes of Y_1, Y_2, and Y_3 band are similar at 380 nm pumping differing from that of the Y_4 band. According to Fig.2 and Fig.3, the $X_1(Y_1)$ band can be attributed to the 1S(e)-1$S_{3/2}$(h) transition of the CdSe core of the sample. Thus it can be considered that the carriers occupy mainly electronic states of the CdS shell under 320 nm pumping, and the e-h pairs are located in the CdSe core under 380 nm pumping. We note here that the energies of the pumping photons are less than the gap energy of ZnS, and thus the ZnS shell is unable to be excited. τ_2 can thus be attributed to the system intrinsic relaxation from the emitting excited states of the CdS shell of the sample.

When we use 320 nm femtosecond pulses to excite the sample, majority of carriers are injected into the CdS shell of the sample and relax from initially populated states to the X_4, X_3, and X_2 bands of the CdS shell. Subsequently, these carriers experience relaxation in the shell with a small quantity of the carriers localizes in the core and directly relaxes to the CdSe core X_1 band. So τ_2 is not observed at the X_1 under 320 nm pumping, but appears in decay trances of the X_2, X_3, and X_4 bands.

When the sample is excited with 380 nm femtosecond pulses, a majority of carriers are localized in the CdSe core. These carriers relax from the initially populated states to the states corresponding to the Y_3, Y_2, and Y_1 bands before relaxation in the core. Small part of the carriers is injected into the CdS shell, which relax from the initially populated states to those of the Y_4 band before relaxations in the shell. As a consequence, τ_2 is observed for the Y_4 band, but not for Y_1, Y_2, and Y_3 bands.

From above discussion we might conclude that $Y_1(X_1)$, Y_2, and Y_3 bleaching peaks are in fact corresponding to CdSe core, whereas X_2, X_3, and $X_4(Y_4)$ bleaching peaks to the CdS shell. The relaxation process of carriers under 320 nm pumping is different from that under 380 nm pumping.

The $\tau_{\rm rise}$ of the same bleaching band (X_1 and Y_1, X_4 and Y_4) is different under 320 and 380 nm pumping, which can be ascribed to the difference in initially populated states. The relaxation time from the initial population under 320 nm pumping to the higher X_4 band and the lower X_2 band is about 390 and 520 fs, respectively, where the carrier relaxation time in the intraband of the CdS shell can be deduced to about 130 fs [22]. While under 380 nm pumping, the carriers relax from the Y_3 band to the Y_1 band in about 400 fs in the CdSe core. The results indicate that the carriers relaxation in the intraband of the shell is comparable to the width of pumping laser pulse (130 fs) which is shorter than that in the core.

τ_4 is in the range of 1.2−1.5 ns, well recognized as a result of interband process. This process can be attributed to the system relaxation from emissive excited states of the CdSe core or the CdS shell. The carrier relaxation time τ_3 is observed for all the bands despite the difference in pumping wavelength, which may presumably be related with Auger relaxation of trapped carrier or the system relaxation.

IV. CONCLUSION

In this work, we report time-resolved nonlinear transmission spectra of the core/shell/shell CdSe/CdS/ZnS quantum dots with femtosecond pump-probe technique. The bleaching $\Delta T/T$ kinetic traces of the sample are found non-exponential with both rise and decay components. Via selectively exciting the core (380 nm) or shell (320 nm) the intra- and inter band relaxation dynamics are revealed in detail. Intraband relaxation is found faster in CdS shell than in CdSe core. The results reveal that a great number of defect states exist in the interface between the CdSe core and the CdS shell, indicating that ultrafast spectroscopy might be a proper tool in studying the interface/surface morphology.

V. ACKNOWLEDGMENTS

This work was supported by the National Natural Science Foundation of China (No.11074003) and the Key Program of Educational Commission of Anhui Province of China (No.KJ2010A132). For the help of Prof. J. L. Zhao at Changchun Institute of Optics, Fine Mechanics and Physics, Chinese Academy of Sciences in sample preparation is greatly appreciated.

[1] V. I. Klimov, J. Phys. Chem. B **104**, 6112 (2000).
[2] A. L. Efros and A. L. Efros, Sov. Phys. Sem. **16**, 772 (1982).
[3] L. Brus, J. Chem. Phys. **79**, 5566 (1983).
[4] L. Brus, Appl. Phys. A **53**, 465 (1991).

DOI:10.1088/1674-0068/24/06/640-646

[5] A. Alivisatos, Science **271**, 933 (1996).
[6] S. J. Rosenthal, J. McBride, and L. C. Feldman, Surf. Sci. Reports. **62**, 111 (2007).
[7] D. V. Talapin, I. Mekis, and H. J. Weller, J. Phys. Chem. B **108**, 18826 (2004).
[8] S. J. Lim, B. Chon, T. Joo, and S. K. Shin, J. Phys. Chem. C **112**, 1744 (2008).
[9] A. W. Shill, C. S. Gaddis, and W. Qian, Nano Lett. **9**, 1940 (2006).
[10] E. A. Dias, S. L. Sewall, and P. Kambhampati, J. Phys. Chem. C **111**, 708 (2007).
[11] M. G. Lupo, F. D. Sala, and G. Lanzani, Nano Lett. **12**, 4582 (2008).
[12] S. Deka, A. Quarta, and L. Manna, J. Am. Chem. Soc. **131**, 2948 (2009).
[13] J. Shah, Solid State Electron **21**, 43 (1978).
[14] A. V. Malko, A. A. Mikhailovsky, and V. I. Klimov, J. Phys. Chem. B **108**, 5250 (2004).
[15] D. H. Son, J. S. Wittenberg, and A. P. Alivisatos, Phys. Rev. Lett. **92**, 127406 (2004).
[16] R. D. Schaller, J. M. Pietryga, and V. I. Klimov, Phys. Rev. Lett. **95**, 196401 (2005).
[17] L. Manna, E. C. Scher, and A. P. Alivisatos, J. Am. Chem. Soc. **124**, 7136 (2002).
[18] D. V. Talapin, R. Koeppe, and H. Weller, Nano Lett. **3**, 1677 (2003).
[19] D. V. Talapin, J. H. Nelson, and A. P. Alivisatos, Nano Lett. **7**, 2951 (2007).
[20] L. Carbone, Nano Lett. **7**, 2942 (2007).
[21] A. Cretí, M. Anni, and M. Lomascolo, Phys. Rev. B **72**, 125346 (2005).
[22] A. Cretí, M. Zavelani-Rossi, and M. Lomascolo, Phys. Rev. B **73**, 165410 (2006).
[23] P. T. Jing, J. L. Zhao, and Y. Masumoto, J. Phys. Chem. C **113**, 13545 (2010).
[24] W. W. Yu, L. H. Qu, and W. Z. Guo, Chem. Mater. **15**, 2854 (2003).
[25] C. Onodera and M. Yoshida, J. Phys. Stud. **14**, 3704 (2010).
[26] M. Sanz, M. A. Correa-Duarte, and A. Douhal, J. Photochem. Photobiol. A **196**, 51 (2008).
[27] C. Burda, S. Link, and M. A. El-Saye, J. Phys. Chem. B **103**, 10775 (1999).
[28] V. Klimov, P Haring, and H. Kurz, Phys. Rev. B **53**, 1463 (1996).

DOI:10.1088/1674-0068/24/06/640-646